

Primordial Black Holes and microlensing

Mimoza Hafizi, Lindita Hamolli

University of Tirana, Albania

1st General Meeting of COST Action COSMIC WISPerS

5-8 September 2023

Centro Polifunzionale Studenti, Bari, Italy

Black Holes

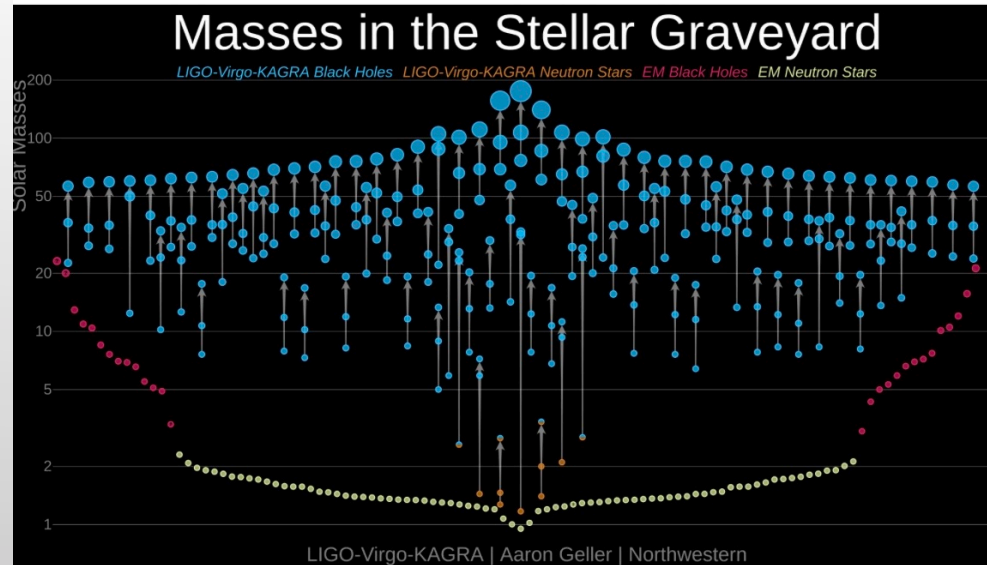
Schwarzschild radius= $2GM/c^2$

Stellar BH (from several up to several tens of solar masses): 28 discovered by electromagnetic telescopes and 240 by gravitational telescopes (2 collapsing and one merged);

Supermassive black holes in centers of large galaxies (10^6 - 10^{11} solar masses);

Intermediate black holes (above 100 solar masses): several from gravitational telescopes and signs from other experiments (GRB lensing).

Primordial Black Holes are hypothetical types of BH formed soon after the inhomogeneous Big Bang.



Black Holes and Neutron Stars discovered via electromagnetic and gravitational telescopes (Image credit: Ligo-Virgo/ Aaron Geller/ Northwestern)

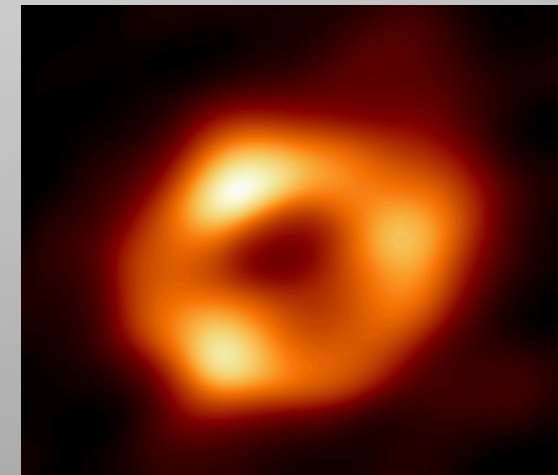


Image obtained by Event Horizon Telescope, published on 12 May 2022, of the **supermassive BH** at the center of the **Milky Way** (4.15×10^6 solar masses).

Formation of PBH and their masses

(Hawking, 1971, MNRAS, 152, 75)

(Carr&Hawking, 1974, MNRAS, 168 (2), 399)

Heuristic treatment. A **comoving volume** V inside the early universe.

Potential energy: $G\rho^2 V^{5/3}$; **Kinetic energy** of expansion: $\rho V^{5/3}(\dot{V}/V)^2$

In a flat universe (Friedmann equations): $(\dot{V}/V)^2 \propto G\rho_m$

Any local increase in density, ρ_0 , could stop the expansion.

Internal energy (radiation era): $\rho c^2 V$.

Condition for collapse, (potential energy higher than internal): $V > (c^2/G\rho)^{3/2}$.

Condition for a BH (R under Schwarzschild radius): $M \propto (c^6/G^3\rho_0)^{1/2}$

Evolution of density in early universe (radiation-dominated era): $\rho \propto T^4$

PBH mass: $M \propto 1/T^2$

Or
$$M \approx \frac{c^3 t}{G} \approx 10^{15} \left(\frac{t}{10^{-23} \text{s}} \right) \approx 10^5 \left(\frac{t}{1 \text{s}} \right) M_s$$

An **enormous mass range**: PBHs formed at the Planck time (10^{-43}s) \rightarrow the Planck mass 10^{-5} g; PBHs formed at 1 s \rightarrow $10^5 M_s$; And further on.

If they exist

Might lead to various interesting astrophysical consequences:

Provide seeds for supermassive black holes in galactic nuclei;

Influence the generation of large-scale structure;

Provide a *fraction* of the **dark matter**.

DARK MATTER

Accounts for about 85% of the matter in the universe;

Interacts with baryonic matter and radiation only through gravity.

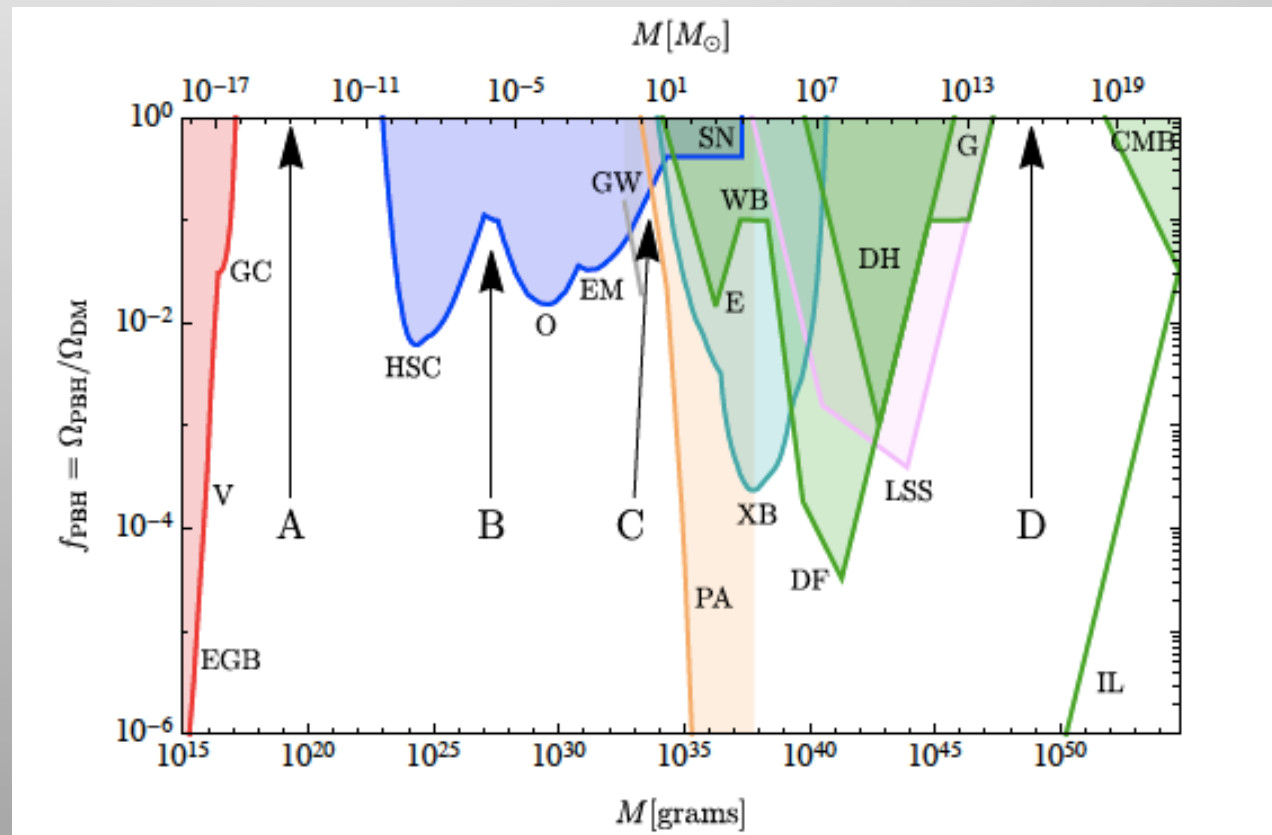
What's the value of $f(M)$, the *fraction* of this dark matter in PBHs of mass M ?

Observational constraints on $f(M)$

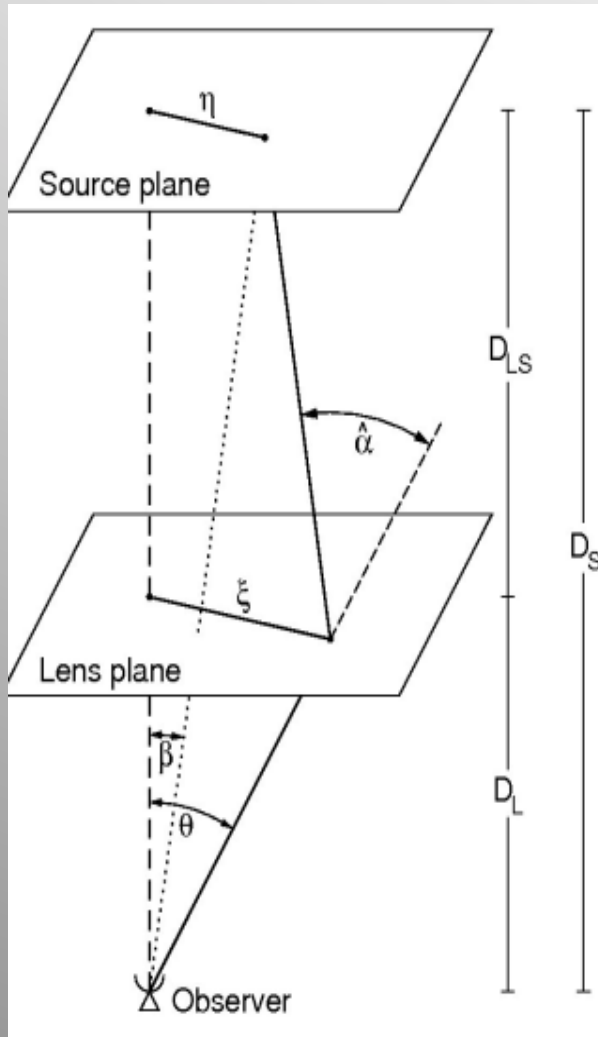
(B. Carr, F. Kühnel, *SciPost Phys. Lect. Notes*, **48**, (2022))

From **evaporations** (red), **lensing** (dark blue), gravitational waves (GW) (brown), **dynamical effects** (green), **accretion** (light blue), **cosmic microwave background distortions** (orange), and **large-scale structure** (purple).

There are four mass windows (A, B, C, D) in which PBHs could have a significant density.



Gravitational Lensing constraints



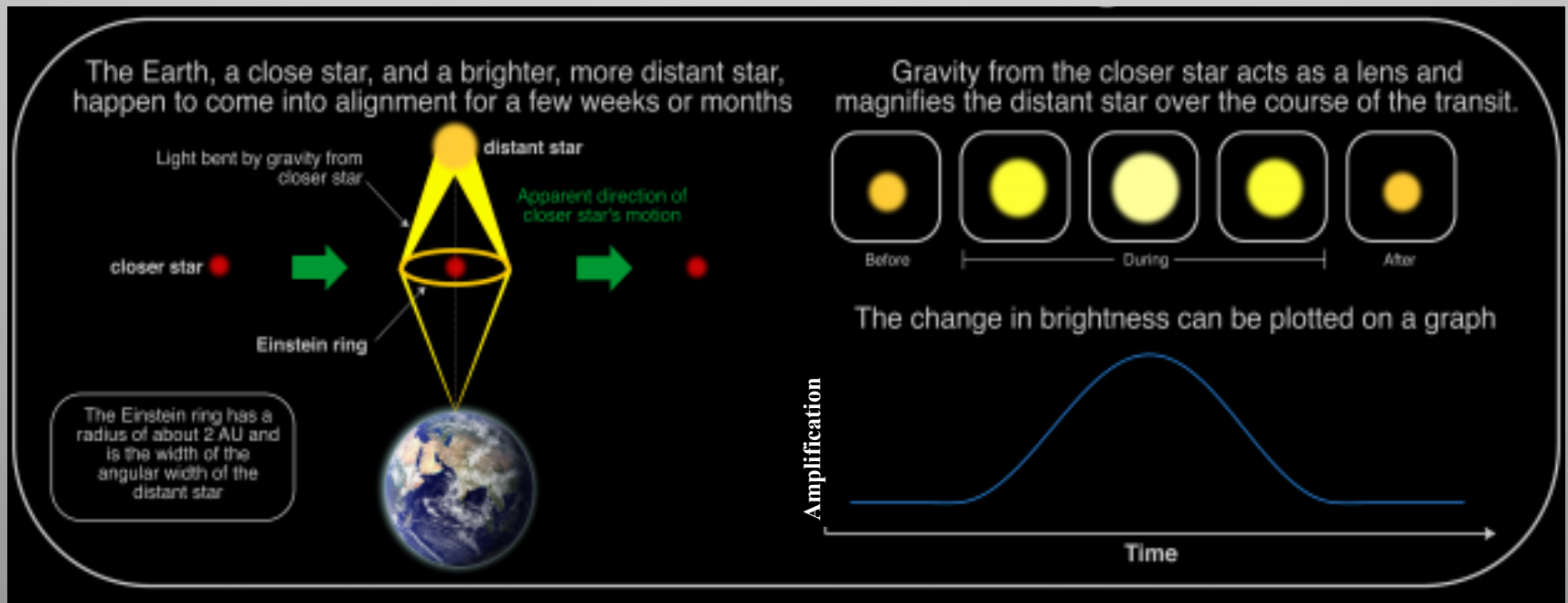
- The **bending of light** by astronomical masses;
- First test of the GR in 1919;
- When lenses are galactic masses: distortions by several arcsecs. **Strong lensing.**

$$\alpha = \frac{4GM}{c^2\xi}$$

$$\theta_E = \sqrt{\frac{4GM(\theta_E)}{c^2} \frac{D_{LS}}{D_S D_L}}$$

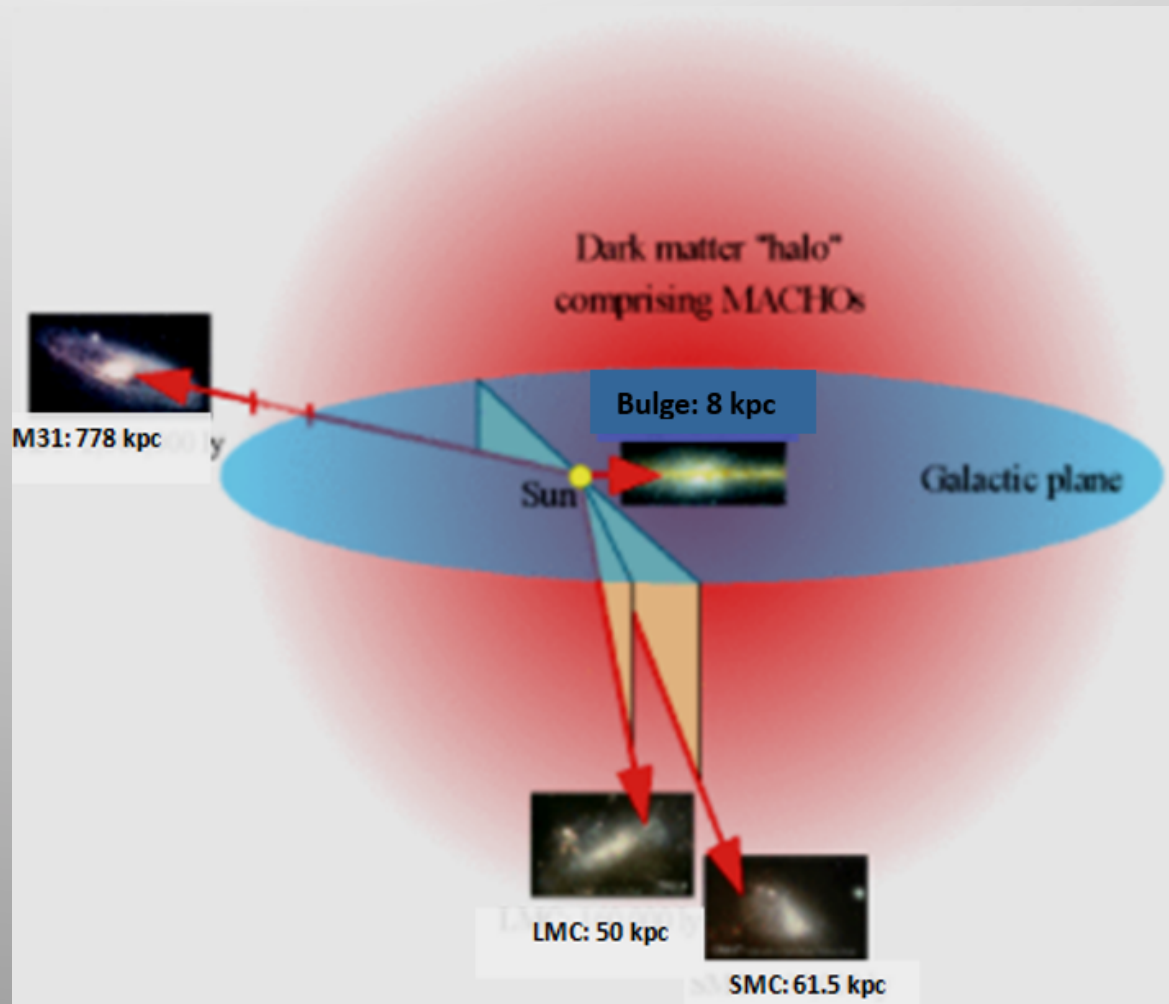
Gravitational microlensing

- Lensing by stellar objects and below;
- The image separation is the order of μ -arcsec, so it cannot be resolved;
- A specific time-dependent amplification of the source brightness;
- **Time-scale** of the event (t_E , Einstein time).



Microlensing observations

- Galactic bulge (8 kpc),
(l,b) \rightarrow $(0^\circ, 0^\circ)$
- LMC (50 kpc)
(l,b) \rightarrow $(280.5^\circ, -32.8^\circ)$
- SMC (61.5 kpc)
(l,b) \rightarrow $(307^\circ, -46^\circ)$
- M31 (778 kpc)
(l,b) \rightarrow $(121.17^\circ, -21.57^\circ)$



Microensing missions

Kepler Data (toward stars in a kiloparsec of distance) obtained during two years of observations.

Subaru Suprime-Cam (HSC), telescope 8.2 m in Mauna Kea, 2019. By monitoring tens of millions of stars.

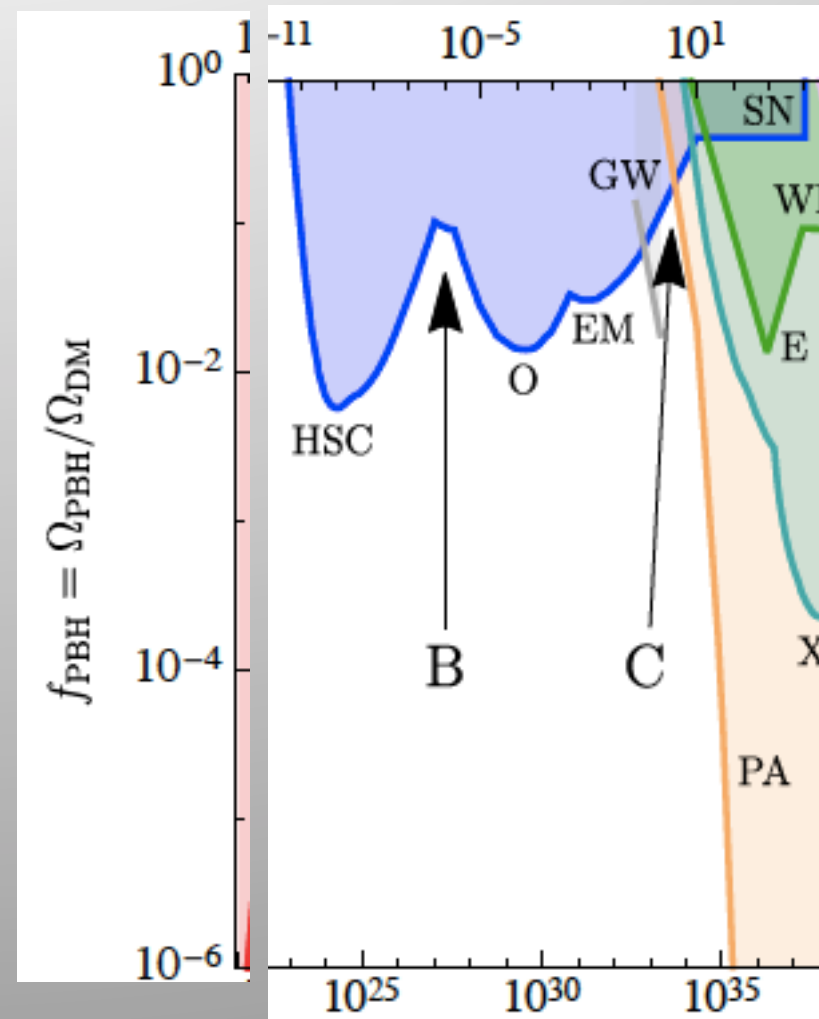
EROS (1996-2004 telescope in the ESO site) measurements towards Galactic Bulge, Light curves of 5.6×10^6 clump giant stars distributed over 66 deg² of the Bulge were monitored during seven Bulge seasons.

Macho: 5.7 years of LMC observations. 1,27 m telescope in Australia. 1992-1999.

OGLE (1992-now, four phases, 1m and 1,3m telescope-Las Campagnas; LMC, SMC and Galactic bulge).

Gravitational microlensing constraints

- **Kepler** Source Microlensing Data (no event) and **Subaru/HSC Andromeda** observations-one event (**HSC**);
- **EROS** and **MACHO** measurements towards Galactic Bulge-120 events (**EM**);
- **OGLE** measurements toward **LMC**-two+two events, and **SMC**-one+three events (**O**);
- Gravitational lensing of **type Ia supernovae** would magnify them and affect the probability distribution of their magnification (**SN**).



OGLE IV observations (Galactic bulge)

Mróz, Przemek, et al. 2019

- 7 years of observations (2010-2017);
- A sample of **8000** gravitational microlensing events;
- 121 fields located toward the Galactic bulge, covering an area of over 160 deg²;
- Optical Depth.

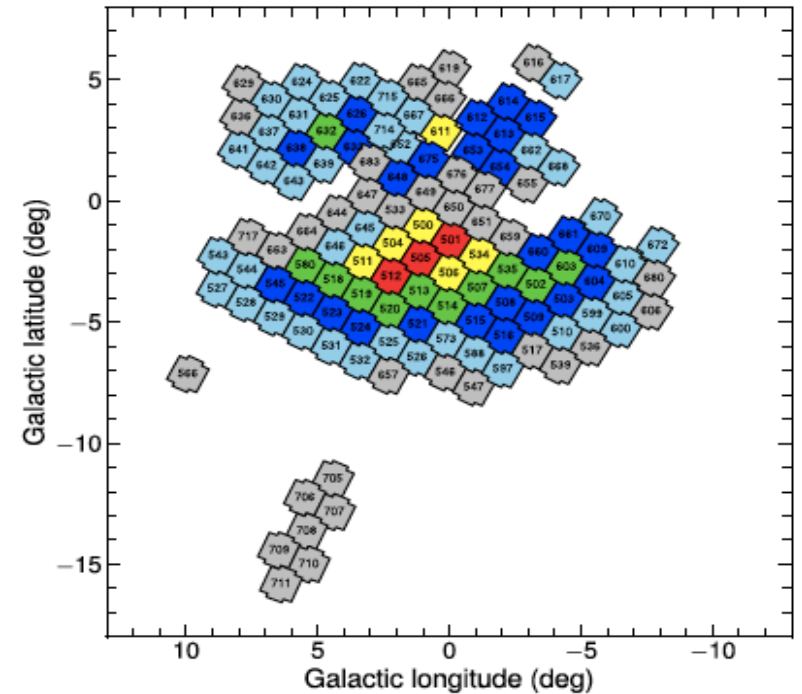


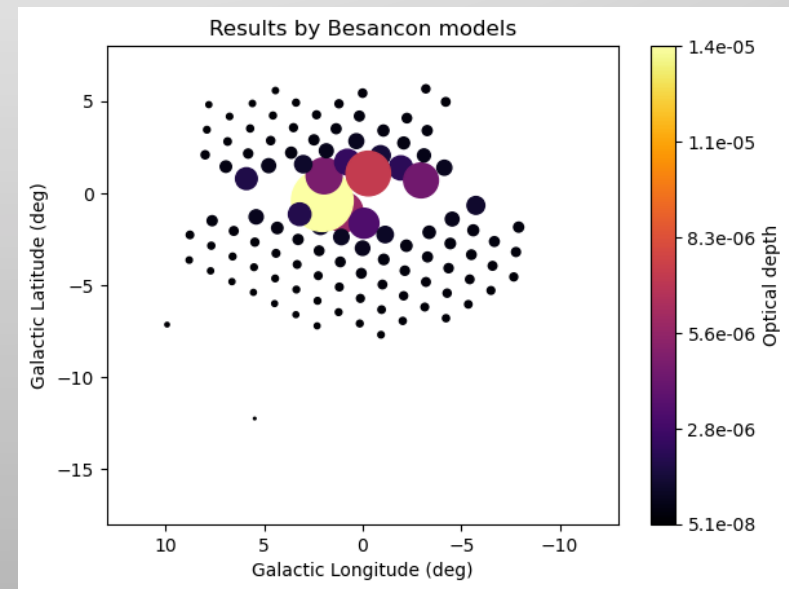
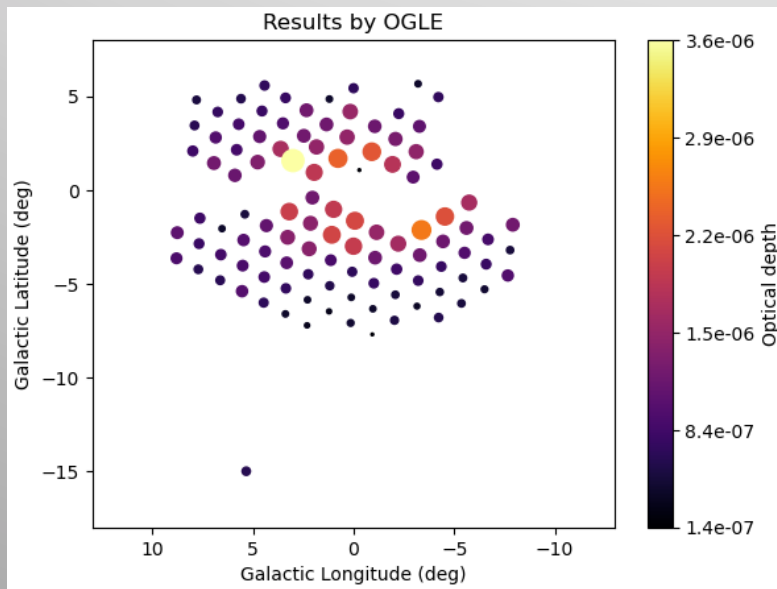
Figure 1. OGLE-IV fields toward the Galactic bulge. Colors mark the typical cadence of observations: red—one observation every 20 minutes, yellow—one observation every 60 minutes, green—two to three observations per night, blue—one observation per night, cyan—one observation per 2 nights. Silver fields were regularly observed during 2010–2013, usually once every 2–3 days.

$$\tau(D_s) = \frac{4\pi G}{c^2} \int_0^{D_s} \rho(D_l) \frac{D_l(D_s - D_l)}{D_s} dD_l$$

$$\tau = \frac{\pi}{2N_* T_{\text{obs}}} \sum_i^{N_{\text{ev}}} \frac{t_{Ei}}{\epsilon(t_{Ei})}$$

OGLE IV observations versus models

Here we compare the observational results with numerical ones, based on theoretical models (Besançon model) for star distributions.



Left: Diagrams with the values of the optical depth, found in 121 channels of OGLE IV observations (colors and surfaces of circles indicate the value)

Right: Numerical values (stars: 7 thin disk and thick disk; bar; halo).

Besaçon Model

Thin disk

$$\rho_d = \rho_0 \left[\exp \left(-\sqrt{0.25 + \left(\frac{a}{R_d} \right)^2} \right) - \exp \left(-\sqrt{0.25 + \left(\frac{a}{R_h} \right)^2} \right) \right]$$

$$a^2 = r^2 + \left(\frac{z}{\epsilon} \right)^2$$

$$R_d = 2170 \text{ pc}$$

$$R_h = 1330 \text{ pc}$$

Thick disk

$$\rho(r, z) = \rho_0 \exp \left(\frac{r_\odot - r}{h_R} \right) \begin{cases} 1 - \left(\frac{z^2}{\xi(2h_z + \xi)} \right) & \text{for } z \leq \xi \\ \frac{2h_z}{2h_z + \xi} \exp \frac{\xi - |z - z_\odot|}{h_z} & \text{for } z > \xi \end{cases}$$

$$h_z = 533.4 \text{ pc}$$

$$h_R = 2355.4 \text{ pc}$$

$$\xi = 658 \text{ pc}$$

Bar

$$\rho(x, y, z) = \rho_0 \operatorname{sech}^2(-R_s(x, y, z))$$

$$R_s(x, y, z)^{C_\parallel} = \left[\left| \frac{x}{x_0} \right|^{C_\perp} + \left| \frac{y}{y_0} \right|^{C_\perp} \right]^{\frac{C_\parallel}{C_\perp}} + \left| \frac{z}{z_0} \right|^{C_\parallel}$$

$$x_0 = 1.46 \text{ kpc}$$

$$y_0 = 0.49 \text{ kpc}$$

$$z_0 = 0.3 \text{ kpc}$$

$$C_\parallel = 0.5$$

$$C_\perp = 3.007$$

Halo

$$\rho(r, z) = \begin{cases} C_1 a^{-2.44} & \text{for } a > 500 \text{ pc} \\ C_1 500^{-2.44} & \text{for } a < 500 \text{ pc} \end{cases}$$

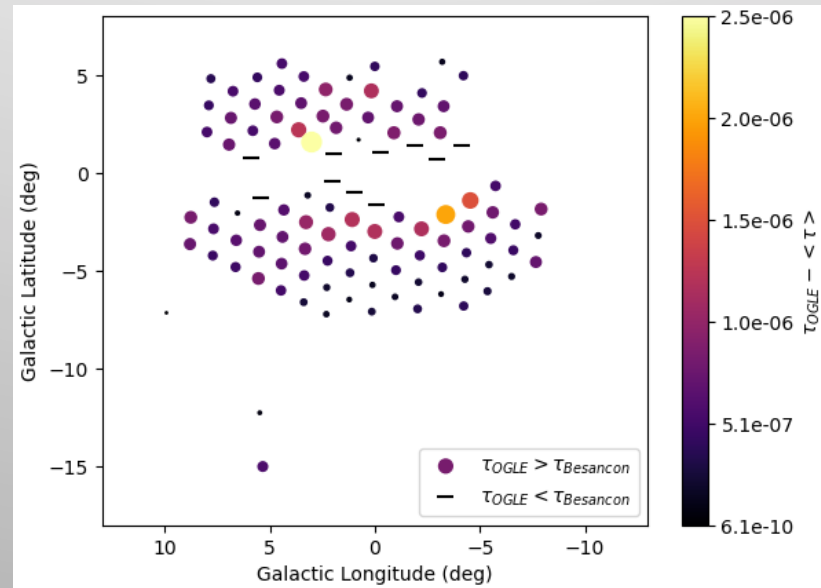
$$a = \sqrt{R^2 + \left(\frac{z}{q_{\text{stell}}} \right)^2}$$

$$q_{\text{stell}} = 0.76$$

$$\rho(R_0, 0) = 9.32 \times 10^{-6} M_\odot \text{ pc}^{-3}$$

OGLE IV observations and the Dark Matter

Here we show the map of the optical depth values for the DM (OGLE IV observations – numerical values for stars);



Optical depth of the order of 10^{-6} .

Further analysis.

Our PREVIOUS STUDIES

About microlensing optical depth and rates for free-floating planets towards the **Kepler's field of view**"

Estimating finite source effects in microlensing events due to free-floating planets with the **Euclid survey**

Investigating the free-floating planet mass by **Euclid observations**

Predictions on the detection of the free-floating planet population with **K2** and **Spitzer** microlensing campaigns

Gravitational microlensing constraints on primordial black holes by **Euclid**

Mimoza Hafizi, Lindita Hamolli

University of Tirana, Albania

THANK YOU!

Refs. For the slide 9

Kepler: K. Griest, A. Cieplak and M. Lehner, *New Limits on Primordial Black Hole Dark Matter from an Analysis of Kepler Source Microlensing Data*, *Phys. Rev. Lett.* 111(18), 181302 (2013), doi:10.1103/PhysRevLett.111.181302.

Subaru/HSC Andromeda: H. Niikura et al., *Microlensing constraints on primordial black holes with Subaru/HSC Andromeda observations*, *Nat. Astron.* 3(6), 524 (2019).

EROS: C. Hamadache et al., *Galactic Bulge microlensing optical depth from EROS-2*, *Astron. astrophys.* 454, 185 (2006), doi:10.1051/0004-6361:20064893, astro-ph/0601510.

OGLE measurements toward LMC: L. Wyrzykowski et al., *The OGLE View of Microlensing towards the Magellanic Clouds. I. A Trickle of Events in the OGLE-II LMC data*, *Mon. Not. Roy. Astron. Soc.* 397, 1228 (2009), doi:10.1111/j.1365-2966.2009.15029.x, 0905.2044.

SMC: L. Wyrzykowski et al., *The OGLE View of Microlensing towards the Magellanic Clouds. II. OGLE-II SMC data*, *Mon. Not. Roy. astron. Soc.* 407, 189 (2010), doi:10.1111/j.1365-2966.2010.16936.x, 1004.5247.

Refs. For Besançon model

Robin, Annie C., et al. "A synthetic view on structure and evolution of the Milky Way." *Astronomy & Astrophysics* 409.2 (2003): 523-540: **Thin disc, 7 components**

Robin, Annie C., et al. "Stellar populations in the Milky Way bulge region: towards solving the Galactic bulge and bar shapes using 2MASS data." *Astronomy & Astrophysics* 538 (2012): A106: **Bar**

Robin, A. C., et al. "Constraining the thick disc formation scenario of the Milky Way." *Astronomy & Astrophysics* 569 (2014): A13: **Thick disc**

Awiphan, Supachai, Eamonn Kerins, and Annie C. Robin. "Besançon Galactic model analysis of MOA-II microlensing: evidence for a mass deficit in the inner bulge." *Monthly Notices of the Royal Astronomical Society* 456.2 (2016): 1666-1680.

Robin, A. C., et al. "A self-consistent dynamical model of the Milky Way disc set to Gaia data." *arXiv preprint arXiv:2208.13827* (2022): **Halo**